PLOS ONE

RESEARCH ARTICLE

Microglia-secreted TNF-α affects differentiation efficiency and viability of pluripotent stem cell-derived human dopaminergic precursors

Shirley D. Wenker[1], María Isabel Farias[1], Victoria Gradaschi[1¤], Corina Garcia[1], Juan Beauquis[2,3], María Celeste Leal[1], Carina Ferrari[1], Xianmin Zeng[4], Fernando J. Pitossi[1]*

1 Fundación Instituto Leloir—IIBBA-CONICET, Buenos Aires, Argentina, **2** Instituto de Biología y Medicina Experimental, CONICET, Buenos Aires, Argentina; Departamento de Química Biológica, Facultad de Ciencias Exactas y Naturales, Universidad de Buenos Aires, Argentina, **3** Universidad de Buenos Aires, Buenos Aires, Argentina, **4** RxCell, Novato, CA, United States of America

¤ Current address: Facultad de Ciencias Exactas y Naturales, Departamento de Química Biológica, Universidad de Buenos Aires (UBA), Buenos Aires, Argentina
* fpitossi@leloir.org.ar

Citation: Wenker SD, Farias MI, Gradaschi V, Garcia C, Beauquis J, Leal MC, et al. (2023) Microglia-secreted TNF-α affects differentiation efficiency and viability of pluripotent stem cell-derived human dopaminergic precursors. PLoS ONE 18(9): e0263021. https://doi.org/10.1371/journal.pone.0263021

Editor: Anju Vasudevan, Huntington Medical Research Institutes, UNITED STATES

Received: January 5, 2022

Accepted: August 19, 2023

Published: September 26, 2023

Data Availability Statement: All relevant data are within the manuscript and/or Supporting information files. There are no gels and blots images/figures in your study and therefore no uncropped, unadjusted images of gels or blots are submitted.

Funding: This research project was funded by the Agencia Nacional de promoción de la investigación, el desarrollo tecnológico y la innovación (http://www.agencia.mincyt.gob.ar/) through grant PICT-

Abstract

Parkinson's Disease is a neurodegenerative disorder characterised by the progressive loss of dopaminergic cells of the *substantia nigra pars compacta*. Even though successful transplantation of dopamine-producing cells into the striatum exhibits favourable effects in animal models and clinical trials; transplanted cell survival is low. Since every transplant elicits an inflammatory response which can affect cell survival and differentiation, we aimed to study *in vivo* and *in vitro* the impact of the pro-inflammatory environment on human dopaminergic precursors. We first observed that transplanted human dopaminergic precursors into the striatum of immunosuppressed rats elicited an early and sustained activation of astroglial and microglial cells after 15 days' post-transplant. This long-lasting response was associated with Tumour necrosis factor alpha expression in microglial cells. *In vitro*, conditioned media from activated BV2 microglial cells increased cell death, decreased Tyrosine hydroxylase-positive cells and induced morphological alterations on human neural stem cells-derived dopaminergic precursors at two differentiation stages: 19 days and 28 days. Those effects were ameliorated by inhibition of Tumour necrosis factor alpha, a cytokine which was previously detected *in vivo* and in conditioned media from activated BV-2 cells. Our results suggest that a pro-inflammatory environment is sustained after transplantation under immunosuppression, providing a window of opportunity to modify this response to increase transplant survival and differentiation. In addition, our data show that the microglia-derived pro-inflammatory microenvironment has a negative impact on survival and differentiation of dopaminergic precursors. Finally, Tumour necrosis factor alpha plays a key role in these effects, suggesting that this cytokine could be an interesting target to increase the efficacy of human dopaminergic precursors transplantation in Parkinson's Disease.

2018-00517 to FJP. Founds were also provided by René Barón Foundation to FJP and the International Society of Neurochemistry -Committee for Aid and Education in Neurochemistry (ISN-CAEN) to SDW. The funders had no role in study design, data collection and analysis, decision to publish, or preparation of the manuscript.

Competing interests: The authors have declared that no competing interests exist.

Introduction

Neurological disorders are one of the main causes of disability in the world. Among these disorders, Parkinson's disease (PD), affects the second largest group of people and has the highest growth in incidence. From 1990 to 2015, the prevalence of PD and, therefore, disability and cause of death doubled, with a prevalence of 98 cases of PD per 100,000 individuals, representing a 15.7% increase [1].

PD is a neurodegenerative disorder, whose cardinal pathology is the loss of dopaminergic (DA) neurons in the *substantia nigra pars compacta*. Current treatments for PD provide symptomatic relief but have side effects in the long term and do not halt disease progression or regenerate DA cell loss [2].

Cell replacement therapy has been proposed as an alternative strategy due to the fact that motor symptoms of PD are caused by the degeneration of a specific cell type, DA neurons. Therefore, grafts of DA precursors (DAp) could have the potential to replace the function of DAn loss and thus reduce the associated motor symptoms. Pre-clinical and clinical trials have provided proof of concept that the transplantation of DA neuroblasts in the striatum can alleviate parkinsonian symptoms [3,4]. DA neuroblasts and not mature DA neurons are used since the transplanted cells need to engraft in the host parenchyma in order to survive. Although the results from clinical trials have demonstrated that this approach is safe, its efficacy was variable and several undesirable side effects such as graft-induced dyskinesia were reported. Thus, standardisation of several factors is crucial to optimise the efficiency of the treatment and try to prevent unwanted effects [3,5]. One important factor for the development of an effective therapy of cell replacement is the host-primary response related to the graft. The microenvironment generated by the host could have dramatic effects on the survival, differentiation and proliferation of the transplanted cells. In this context, microglia activation dramatically affects the host environment after a mechanical intervention to the central nervous system (CNS). Cellular transplantation in the CNS not only includes such a mechanical injury but also provides a plethora of inflammatory and immune stimuli to the transplantation site [6]. Adaptive immune responses are usually prevented by immunosuppression treatments. However, innate immune responses should remain active after transplantation but scarce information is available on its characteristics, duration and functional effects on the transplant. In particular, the possible effects of microglia, the main effectors of the innate immune response in the brain, on the fate of the transplanted cells are poorly described. Microglial activation produces several pro-inflammatory factors with neurotoxic effects (i.e, Tumour necrosis factor alpha (TNF-α), Interleukin (IL)-1, IFN-gamma, Nitric oxide, and reactive oxygen species) that could compromise the viability and/or differentiation of DA precursors [7]. Because grafting to the CNS inevitably causes activation of the host's microglia, understanding its functional effects on the viability and differentiation of DA precursors is important in order to detect potential molecular targets to improve the efficacy of cell therapy.

In this work, we found that sustained and increased microglial and astroglial response were observed 15 days' post-transplantation even in the presence of a constant immunosuppressive treatment. On the contrary, the transplanted cells elicited only a marginal and transient infiltration of neutrophils. Then, we observed that *in vitro*, activated microglial-derived conditioned media diminished human DAp survival, differentiation and affected cell morphology. These effects were blocked by inhibiting TNF-α in the culture.

Materials and methods

Reagents

All chemicals used were of analytical grade. D-MEM, αMEM; GMEM, Neurobasal, B27, Geltrex, Acutase, penicillin/streptomycin; NEAA; β-mercaptoethanol and KSR were obtained from Gibco. GDNF and BDNF were from Peprotech. L-glutamine; Na pyruvate; dimethylsulfoxide; Mitomicym C; lipopolysaccharide and p-formaldehyde (PFA) were obtained from Sigma-Aldrich. TNF-α -ELISA Kit was obtained from BD. Triton X-100 and Tween 20 were from Merck. Fetal bovine serum (FBS), and were obtained from Internegocios SA (Argentina). Cyclosporine was from Novartis.

Cell cultures

PA6 cells. Mouse stromal cell line PA6 (RIKEN BRC) were maintained and propagated αMEM, supplemented with 10% FBS and antibiotics (100 U/ml penicillin, 100 μg/ml streptomycin).

Human Neural Stem Cells (hNSCs). hNSCs-H14, kindly gifted by Dr Xianmin Zeng were propagated using Neurobasal medium supplemented with B27, 2 mM NEAA, 20 ng/mL of bFGF and antibiotics (100 U/ml penicillin, 100 microg/ml streptomycin) on Geltrex-coated dishes. Quality control for hNSCs populations were analysed by immunofluorescences for Nestin and SOX-1. The hNSC used in this study were derived from hESC line H14 via the neural patterning/floor plate stage by sonic hedgehog [8]. The dopaminergic neurons differentiation from hESC-derived NSC were shown to be authentic dopaminergic neurons and survived/engrafted after transplantation (co-expressing TH and FoxA2/Lmx1a) [9].

Dopaminergic differentiation. Generation of PA6 conditioned media (PA6-CM): PA6 cells were cultured, grown to 80% confluence, and then treated with Mitomycin C (0.01mg/ml; 2 hs). After 5 washes with PBS, PA6 cells were incubated with fresh PA6 culture medium for 16 h. Then, PA6 maintenance culture medium was replaced with ESD medium (GMEM with 10% KSR, 1× NEAA, 1× Na pyruvate, and 1× β-mercaptoethanol). PA6-CM was collected every 24 h during 1 week [10].

DA differentiation was initiated by culturing hNSCs with PA6-CM on culture dishes coated with poly-L-ornithine (20 μg/mL) and laminin (10 μg/mL). After 14 days of differentiation, DA precursors (DA14) (150000 live cells/cm2) were transferred to 24-well plates. Cells were cultured in PA6-CM with BDNF (20 ng/mL) and GDNF (20 ng/mL) until day 28 (DA28) [10].

The different states of maturation from hNSCs cultures to dopaminergic differentiation were analysed macroscopically and by immunofluorescent staining of differentiation markers such as TH, Foxa-2, LMX1a, TUJ1, GFAP. The characterization was carried out at two stages of the differentiation protocol: day15 (DA15) and day 28 (DA28) [11].

In vitro treatments were carried out after 24 h of incubation of DA14 cultures.

BV2 microglial cells. Mouse BV2 microglial cell line was provided by Dr. Guillermo Giambartolomei (Hospital de Clínicas, Buenos Aires, Argentina). Cell line was maintained in 100 mm plastic tissue-culture dishes (GBO) containing D-MEM supplemented with 2 mM L-glutamine, antibiotics (100 U/ml penicillin, 100 microg/ml streptomycin), 10% FBS [12].

All cultures were developed at 37˚C with 5% CO_2 and 100% humidity. Media were replaced every 2 days and cells were split before they reached confluence.

Animals. Adult male Wistar rats (Jackson Laboratory, Bar Harbor, ME, USA), bred for several generations in the Leloir Institute Foundation facility, were used in all of the experiments. The animals were housed under controlled temperature conditions (22±2˚C), with food and water provided ad libitum and a 12:12 dark:light cycle with lights on at 08.00 h. All

experimental procedures involving animals and their care were conducted in full compliance with NIH and internal Institute Foundation Leloir guidelines and were approved by the Institutional Review Board "Cuidado y Uso de Animales de Laboratorio (CICUAL-FIL)". All of the animal groups were periodically monitored, indicating that the welfare of the animals was consistent with the standards of the ethical guidelines for animals.

Cell transplantation. For stereotaxic injections, the animals were anaesthetized with ketamine chlorhydrate (80mg/kg) and xylazine (8mg/kg). Intrastriatal stereotaxic transplantation was conducted on cyclosporine A-immunosuppressed male rats (age: 8 weeks). The stereotaxic coordinates were: bregma +1.0 mm; lateral +3.0 mm; ventral -5 and –4.5 mm [13]. After confirmation of the viability of the hDAp with Trypan blue vital stain, the concentration of the suspension was adjusted to 125000 cell/μL. About 250000 human DAp (viability: 81%) derived from hNSCs-H14 or saline solution were transplanted into the left striatum by using a Hamilton syringe [14]. 2 μl of the cell suspension was inoculated. The injection flow was 0.5μl/min. After injection, the cannula was held in place for 5 min, before being slowly retracted. The experimental animals did not show signs of ongoing disease. They presented with normal fur, activity, movement, and food consumption.

Cyclosporine A (Novartis, 15 mg/kg) was administered daily (Intraperitoneal injection) until the end of the experiment, starting 2 days before cell transplantation [15].

Host primary responses related to the graft were analysed by histological and immunofluorescence techniques at different time points (1, 7, 15 and 28 days. $n = 5$ rats per group), except for cytokine expression analysis that was performed only at day 28 post-grafting. In this case, the male rat was the experimental unit.

An aliquot of hDAp obtained from transplantation was cultured for terminal differentiation *in vitro*. At DA28, 17±1% of Tyrosine hydroxylase (TH)-positive cells were detected by immunofluorescence.

In vitro experimental treatments

A. Microglia activation: BV2 cells were seeded in a 6-wells plate (75000 cells/cm2). After 24 h, cell cultures were treated with lipopolysaccharide (LPS) for 24 h according to Dai and colleagues [12].

B. DA precursors acute exposure to conditioned media from microglial cells: DA precursors had been previously plated for 24 h, as DA14, in 0.5 ml of PA6 medium containing differentiation factors. Activation of BV2 microglial cells (24 h) were carried out as explained before. After centrifugation (2000 rpm, 10 minutes) 0.6 ml cell-free supernatants (CM, conditioned media) from basal and activated microglial cultures were transferred to wells containing DA precursors (DA15). After 4 days of DA precursor incubation with conditioned medium from BV2 cells (CM-BV2), evaluation of cell survival and differentiation was performed.

In TNF-α neutralisation experiments etanercept (Enbrel, Pfizer; 100 ng/mL) [16], an inhibitor of both soluble and transmembrane forms of TNF, was added to CM-BV2 as co-treatment.

Measurement of nitric oxide

Nitric oxide (NO) production was determined by measuring the accumulation of nitrite, the stable metabolite of NO, in culture medium. Isolated supernatants collected from microglial cell cultures exposed to LPS for the indicated period were mixed with equal volumes of the Griess reagent (1% sulfanilamide, 0,1% naphthylethylenediamine-dihydrochloride, and 2%

phosphoric acid) and incubated at 25˚C for 10min. Absorbance at 540 nm was measured in a microplate reader [17].

Cytokine quantification

TNF-α was measured by enzyme-linked immunosorbent assay (ELISA) in supernatants obtained as described above for NO measurement. ELISA test was performed according to the manufacturer's instructions of the kit. In each trial, samples were analysed in duplicate against standards of known concentration.

Histology

The animals were deeply anaesthetized as previously described (16) and were transcardially perfused with heparinized saline, followed by ice-cold 4% PFA in phosphate buffer (PB) (0,1M; pH 7,2). Brains were dissected and placed in the same fixative overnight at 4˚C and cryoprotected in 30% sucrose 0.1M PB solution. Then, the brains were frozen in isopentane and cut using a cryostat into 40-μm serial coronal sections through the left prefrontal cortex. Sections were mounted on gelatine coated slides and stained with Cresyl Violet to assess the general nervous tissue integrity, neutrophils cell counts and inflammation. For immunohistochemistry, sections were stored in cryoprotective solution at −20˚C until needed.

Immunofluorescence

Free-floating sections were rinsed in 0.1% Triton in 0,1M PB. After washes with PB-T, samples were blocked in 1% donkey serum for 45 min, and then incubated overnight at 4˚C with primary antibodies diluted in blocking solution. The list of antibodies is provided in Table 1. After three 10-minute washes with 0.1 mol/L PB, the sections were incubated with indocarbocyanine (Cy3) or cyanine Cy2 (Cy2)- conjugated donkey anti-rabbit or anti-mouse antibody, respectively (1:500; Jackson ImmunoResearch) for 2 h at room temperature, rinsed in PB and mounted in Mowiol (Calbiochem). 5–6 sections per animal were analysed.

Table 1. List of antibodies used.

Antibody	Trademark	Catalogue numbers
Anti-GFAP	DAKO	Z0334
Anti-MHC-II	Serotec	MCA46G
Anti-ED1	Serotec	MAC341R
Anti-SOX1	R&D system	AF3369
Anti-Nestin	Abcam	ab22035
Anti-TUJ1	Promega	G712A
Anti-MAP-2	Cell Signaling	9043S
Anti-FOXA-2	Abcam	ab117542
Anti-LMX1a	Abcam	ab31006
Anti- Tyrosine hydroxylase (TH)	Pell-Frezze	P40101
Anti-Caspase 3 active (CA3)	Neuromics	RA15046
Anti-NfkB	SCBT	sc-372
Anti-hNCAM	SCBT	sc-33686
Anti-TNF-α	SCBT	sc-1351
Anti-IL-1b	Neuromics	GT15105
Anti-IL-6	Peprotech	500P73

https://doi.org/10.1371/journal.pone.0263021.t001

Digital images were obtained in a Zeiss LSM 510 laser scanning confocal microscope equipped with a krypton-argon laser.

As technical controls for anti-IL1 and IL-6 immunofluorescence, similar coronal samples of brains injected with 3x 10^6 particles of an adenoviral vector expressing IL-1 beta in the pre-frontal cortex, re-stimulated peripherally with 10^9 particles of the same vector and sacrificed 28 days later were used. These treatments allow the expression of brain IL-1 and IL-6 as described in [18]. As negative controls, similar brain samples, but omitting the primary antibody, were used.

DA cell cultures: samples were fixed with PFA in 4% w/v in PBS, with incubation at room temperature (20 min). After three washes with PBS-T, samples were blocked with 1% donkey serum in PBS-T (1h at room temperature), and then incubated with primary antibody (Table 1), for 16hs at 4˚C. After PBS-T washes, incubation with the secondary antibody (1:1000; Jackson ImmunoResearch) were performed proceed for 2 hrs at room temperature in the dark. At the end, excess antibody was removed with three new washes with PBS, nuclear staining will be performed with Hoechst 33258 dye (1:1000 dilution in PBS). After washing thrice with PBS, samples were mounted in Mowiol (Calbiochem).

BV-2 cells: After fixation with methanol, NFκB immunocytochemistry was performed on BV2 cells to determine nuclear translocation as a proxy for cell activation. Cells attached to coverslips were permeabilized with 0.5% triton X-100 in PBS and unspecific binding sites were blocked with 1% BSA in PBS. Cells were incubated with primary antibody against NFκB and then with Alexa Fluor (488/596; Thermo-Fisher) labelled secondary antibodies. Nuclei were visualised Hoechst 33258 dye (1:1000). After washing thrice with PBS, samples were mounted with Mowiol (Calbiochem).

Fluorescence microscopy: Hoechst nuclear staining of apoptotic cells

DA cell cultures were developed on slide covers plated in a 24-well plate. After treatments, cells were fixed with PFA 4% w/v in PBS for 20min at 4˚C, exposed to Hoechst 33258 dye in PBS for 30 min at room temperature, and washed thrice with PBS. Finally, samples were mounted and fluorescent nuclei with apoptotic characteristics were detected and analysed by immunofluorescence microscopy. Apoptotic cells were identified by morphology and nuclear fluorescence intensity. The condensed chromatin within apoptotic cells stains particularly heavily showing blue fluorescence. In addition, little apoptotic bodies released from nuclei are also detected because of their brilliant blue colour. Differential cell count was performed by evaluating at least 1000 cells [17].

Images were captured with Zeiss Axio Observer and Zeiss LSM 510 laser scanning confocal microscope equipped with a krypton-argon laser.

Image analysis

Polymorphonuclear-neutrophil (PMN) cells were identified by their nuclear morphology appearance in 40-μm thick cresyl violet-stained sections. For MHC II-positive and GFAP-positive cell quantification, approximately 10 fields were quantified for each animal using the Zeiss Image J software. The total number of positive cells was normalised to the total area counted for each sample [18].

Twenty images were obtained by random sample and the analysis was performed using the Image J software. Using the image overlay and cell count plugins, the total number of cells per field and the number of cells positive for the corresponding labelling were counted (example: SOX1, Nestin, TH, TUJ1, LMX1a, FOXA-2, GFAP). In this way, the percentage of positive

cells will be obtained in relation to the number of nuclei counted. At least 1000 total cells were counted.

Differentiation analysis

DA precursors were seeded and after 24 h-incubation, DA15 were exposed to CM-BV2. Cell morphology was observed under phase-contrast in an inverted microscope at 200x magnification and photographed by using a Nikon DS-L3 digital camera. Cell differentiation was determined in independent experiments by counting differentiated cells based on morphological criteria [19] and expressed as percentage of total cells (at least 500 cells).

For neurite outgrowth analysis from TH+ cells derived from DA differentiation were performed at DA19 and DA28 stages. Multiple independent images were taken from immunofluorescence against TH at 400x magnification. At least 10 neurites per field were selected for neurite outgrowth measurement and means of neurite length were calculated for each assay. This neurite tracing technique was implemented in the form of a plugin (NeuronJ) for ImageJ, the computer-platform independent public domain image analysis program inspired by NIH-Image [20].

Statistical analysis

Statistical analysis was performed using GraphPad Prism, version 6.00 for Windows (GraphPad Software, San Diego, CA, USA). Results were expressed as mean and standard error (SEM) of n independent trials (at least 3) indicated in each figure. Data were tested for normality (Shapiro–Wilks test) to use parametric or non-parametric statistical analysis.

Statistical significance was calculated using two-tailed Student's t test or ANOVA followed by a *post hoc* multiple comparison test as indicated. When corresponding, statistical differences between groups were assessed by Mann-Whitney test or Kruskal-Wallis One Way Analysis of Variance. At least differences with $P<0.05$ were considered the criterion of statistical significance.

The figures have a resolution of 300 pixels per inch.

Results

Host response to hDAp transplantation

hNSCs expressed over 95% of Nestin and Sox-1, proving that they were *bona fide* hNSC (Fig 1C). Human dopaminergic precursors (hDAp) were obtained by incubating hNSCs with PA6-conditioned medium (PA6-CM) (Fig 1A). We observed morphological changes such as outgrowth of elongated cells (Fig 1B). After 14 days, DA precursors (DA15) expressed characteristic early DA markers such as Foxa-2 (72,6±4,7%) and Lmx1A (66,0±4,0%) and late markers such as Tyrosine hydroxylase (TH) (5,5±0,8%). As expected for such a protocol, at 28 days, cultures contained approximately 19,1±0,9% TH-positive cells; 70,5±7,3% positive cells for the pan-neuronal marker, TUJ1; and less than 5% of glial cells (3,4±0,5% GFAP-positive cells) (Fig 1C).

Different stages of maturation from cultures of hNSCs induced to dopaminergic differentiation were analysed by immunofluorescence. The expression of the following markers were detected and quantified at two stages of the differentiation protocol: Foxa-2, LMX1a and TH for DA15 cells (DA precursors) (n = 6) and TUJI; GFAP and TH for DA28 (n = 5) (Fig 1).

A preparation of 250.000 hDAp with at least 80% living cells was transplanted into the rat striatum. Animals were immunosuppressed with daily injections of cyclosporine A during the

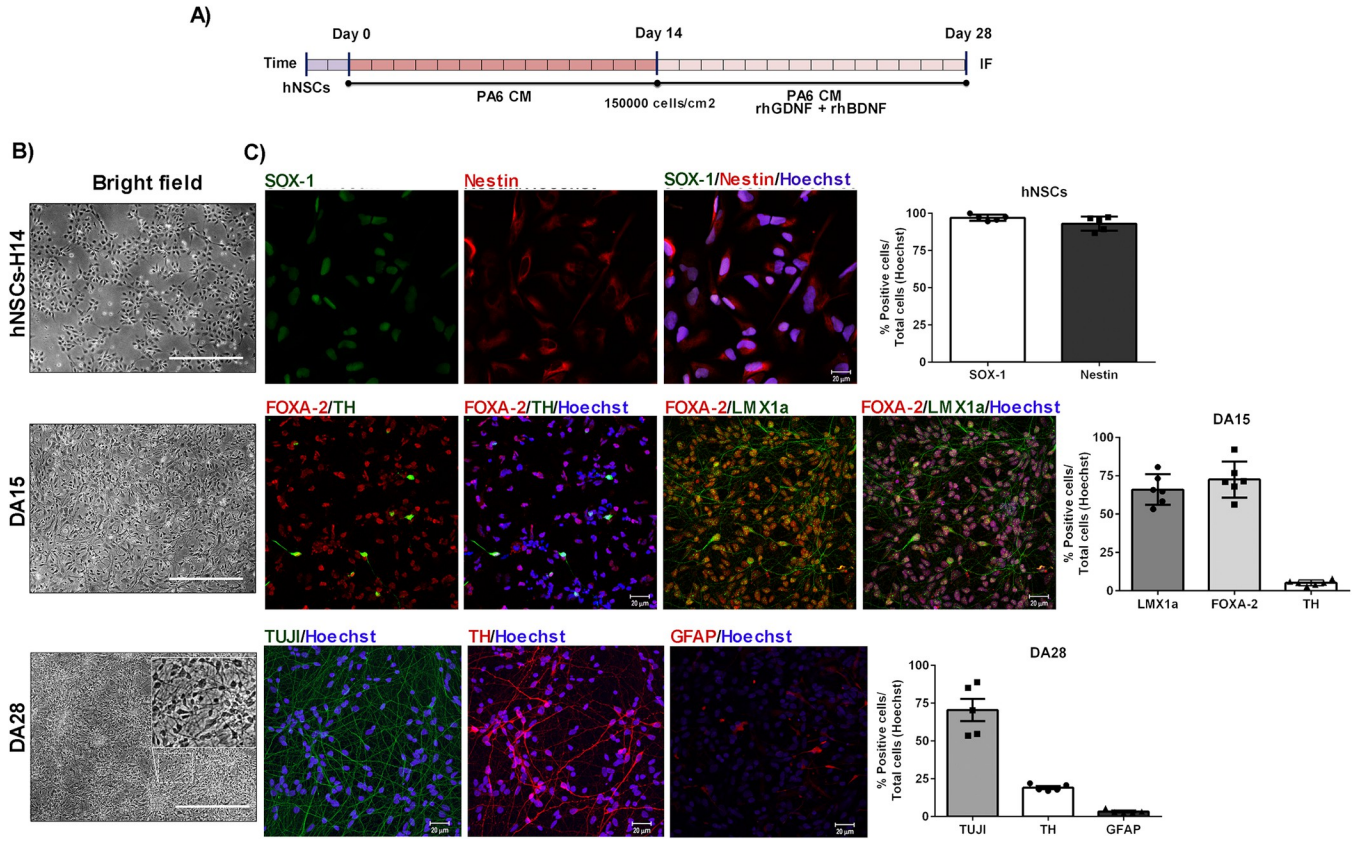

Fig 1. Dopaminergic differentiation from hNSCs. (A) Differentiation protocol was initiated by culturing hNSCs-H14, in PA6-CM for 14 days (Day14). After this period, PA6-CM was supplemented with rhBDNF and rhGDNF for a period of 14 days (DA28). (B). Photographs from each stage showed morphological changes. (C) Quality control for hNSCs populations were analysed by immunofluorescence techniques for Nestin and SOX-1 (n = 5). Cell nuclei were labelled by Hoechst staining. Scale bar are shown in white: 20μm. Each bar represents mean±SEM of independent assays. Magnification: 40X. n = independent experiments.

https://doi.org/10.1371/journal.pone.0263021.g001

total length of the experiment (Fig 2A) (14). Post-mortem evaluation revealed surviving grafts, visualised by the presence of human-specific NCAM staining (Fig 2B).

Histological analysis revealed an early polymorphonuclear neutrophil (PMN) infiltration (1day: 4,04e-4±8.50e-5 Neutrophils/area) from the periphery, which was resolved by 7 days (5,46e-5±2,25e-5 Neutrophils/area. $^{*}p<0,05$ vs. 1 day) (Fig 2C). PMN were identified by their nuclear morphology appearance in 40-μm thick Cresyl violet-stained sections. Astroglial activation as seen by GFAP-staining, increased 7 days after transplantation, reaching a peak at 15 days (1 day: 2,13e-4±2,54e-5 vs. 15 days: 9,76e-4±1,03e-4 GFAP+cells/area. $^{**}p<0.01$), beginning to decay at 28 days (28 days: 8,34e-4±9,58e-5 GFAP+cells/area. $^{*}p<0,05$ vs. 1 day) (Fig 2D and 2E). Transplantation of hDAp in cyclosporine A-daily immunosuppressed rats resulted in microglial activation as demonstrated by the presence of MHC-II+ cells, which specifically label activated microglia [18,21]. MHC-II stained all the activation stages but not resting microglia. According to our results, MHC-II+ cells presented the typical morphology of activated microglial cells: elongated-shaped cell body with long and thicker processes and/or round-shaped body with short, thick and stout processes (Fig 2D). Statistical analysis of microglial activation determined by MHCII-positive cell density showed a marked increase at 15 days (1 day: 6,67e-5±1,32e-5 vs. 15 days: 2,19e-4±1,96e-5 MHC-II+cells/area. $^{*}p<0,05$) which was sustained up to the last time point analysed 28 days: 3,29e-4±2,16e-5 MHC-II+cells/area. $^{**}p<0.01$ vs. 1 day) (Fig 2D and 2F).

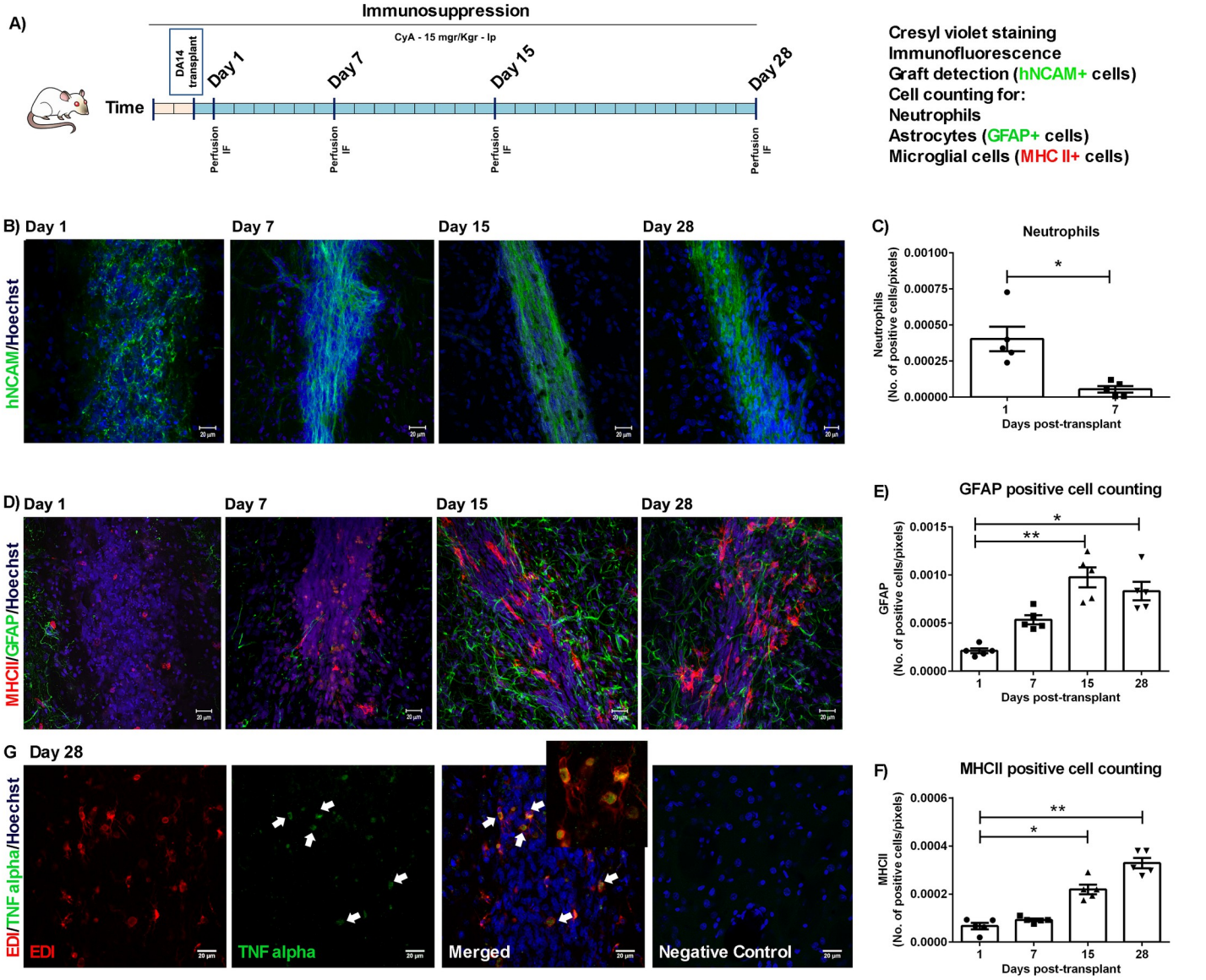

Fig 2. Primary host response related to the graft. (A) DA14 cells were obtained from hNSCs and 250000 cells (viability: 81%) were transplanted into the striatum of immunosuppressed Wistar male rats (age: 8 weeks). At different time points (1, 7, 15 and 28 days) host primary responses related to the graft were analysed by immunofluorescence techniques. (B) Detection of human-specific NCAM (hNCAM) allowed for identification of the graft. (D) Astrocytes (GFAP-positive cells) and activated microglia (MHC-II-positive cells) related to the graft can be observed after 7 days of surgery. (E-F) There is a significant increase in MHC-II+ and GFAP+ cells at 15 and 28 days post-graftment of hDA14 (*p<0,05 and **P<0.01). Kruskal-Wallis ANOVA followed by Dunn's post hoc test, n = 5. (G) Expression of TNF-α by immune fluorescence was observed in EDI positive cells but not in saline-injected animals (Negative control) at Day 28 post surgery (arrows). Inset: Digital zoom of EDI/TNF-α positive cells. Representative pictures of the grafts are shown (Magnification: 40X). Scale bar are shown in white: 20μm. Each bar represents mean±SEM of independent assays. n = 5 rats per group. n = independent experiments.

https://doi.org/10.1371/journal.pone.0263021.g002

Interestingly, tumour necrosis factor alpha (TNF-α) expression was detected 28 days post-transplantation but not after saline injection (Fig 2G). On the contrary, no Interleukin(IL)-1 or IL-6 were observed (S1B Fig). TNF-α expression co-localized with ED1-positive microglial cells within the graft core and the periphery (Fig 2G). These results show that there is a

sustained host response to the transplant in immunosuppressed animals where TNF-α but not two other major pro-inflammatory cytokines are involved.

Conditioned media from microglia have toxic effects on hDAp: short term effects

Previously, we observed a primary response related to the xenograft of hDAp, with a significant increase of microglial activation. As the effects of the host microglial cells on the fate of the transplanted dopaminergic precursors are poorly described, we were interested in simulating the impact of rodent microglial activation on the differentiation and survival of hDAp derived from NSCs.

Microglial activation using bacterial lipopolysaccharide (LPS), was analysed by determining pro-inflammatory mediators such as nitrites (NO) and TNF-α in the cell culture supernatant. LPS led to a significant increase in nitrite production (Basal: 1,2±0,7 vs. Activated (LPS): 31,9 ±1,5 uM. $^{**}p<0.01$) and TNF-α secretion (Basal: 22,3±14,3 vs. Activated (LPS): 739,7±76,1 pg/ml. $^{*}p<0.05$) 24 h after cell activation (Fig 3A and 3B). In addition, NFkB nuclear translocation was also observed in BV2 cell cultures after cell activation (Fig 3C).

In order to analyse the short-term effect of microglial activation on hDAp, we exposed DA15 cultures to conditioned media from BV2 cells (basal–CM-BV2 Basal- or activated condition–CM-BV2 Activated-) until DA19 (Fig 4A). Morphological analysis was performed and cell differentiation was determined by counting neural differentiated cells based on morphological criteria, in which neuron–like-cells were considered in those cells that bear neurites longer than twice the size of the cell body [19].

A decrease in neuron-like cell count (CM-BV2 Basal: 72,8±1,9 vs. CM-BV2 Activated: 57,9 ±2,4%. ***p<0,001. Fig 4B and 4C) and neurite length of TH positive cells was detected in DA precursors cultures incubated with CM from activated microglia (CM-BV2 Basal: 339,0±31,2 vs. CM-BV2 Activated: 148,0±15,4 neurites length. ***p<0,001) (Fig 4B–4E). A significant reduction of TH-immunoreactive cells was detected in DA cultures exposed to CM from activated BV2 compared to basal conditions (CM-BV2 Basal: 5,9±0,4 vs. CM-BV2 Activated: 2,5 ±0,4%TH+cells. ***p<0,001. Fig 4F and 4G). Concomitant with these results, we observed an increment in apoptotic nuclei (CM-BV2 Basal: 7,2±0,7 vs. CM-BV2 Activated: 21,4±2,5% apoptotic cells. **p<0,01. Fig 4I) and caspase activated 3 (CA3)-positive cells (Fig 4H) in DA precursors after 4 days of incubation with CM from activated microglia.

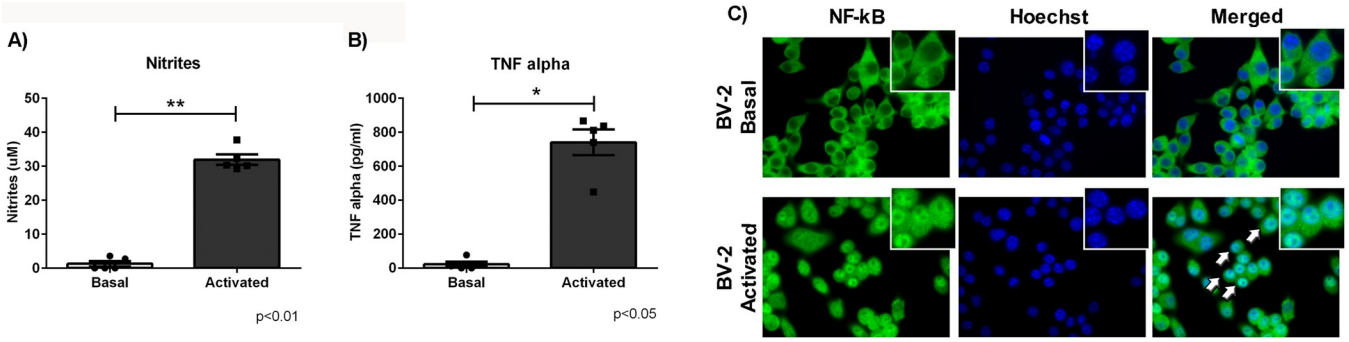

Fig 3. Characterization of microglial cell activation. BV2 cultures were exposed or not (Basal) to LPS (Activated), and parameters of microglial cell activation were determined. (A) Nitrite production (Griess method) and TNF-α secretion (ELISA test) (B) were measured after 24 h of cell activation. Asterisks indicate statistically significant differences: Nitrite, $^{**}p<0.01$ with respect to basal condition (n = 5) and $^{*}p<0.05$ TNF-α with respect to basal condition (n = 5) (Mann-Whitney test). (C) NFkB nuclear translocation was analysed by immunofluorescence after short term exposure to LPS. Significant increases in nitrite and TNF-α were induced by LPS treatment. NFkB nuclear translocation can be seen in BV2 under LPS exposure (arrows) (Magnification: 40X). Values are mean±SEM of independent assays. n = independent experiments.

https://doi.org/10.1371/journal.pone.0263021.g003

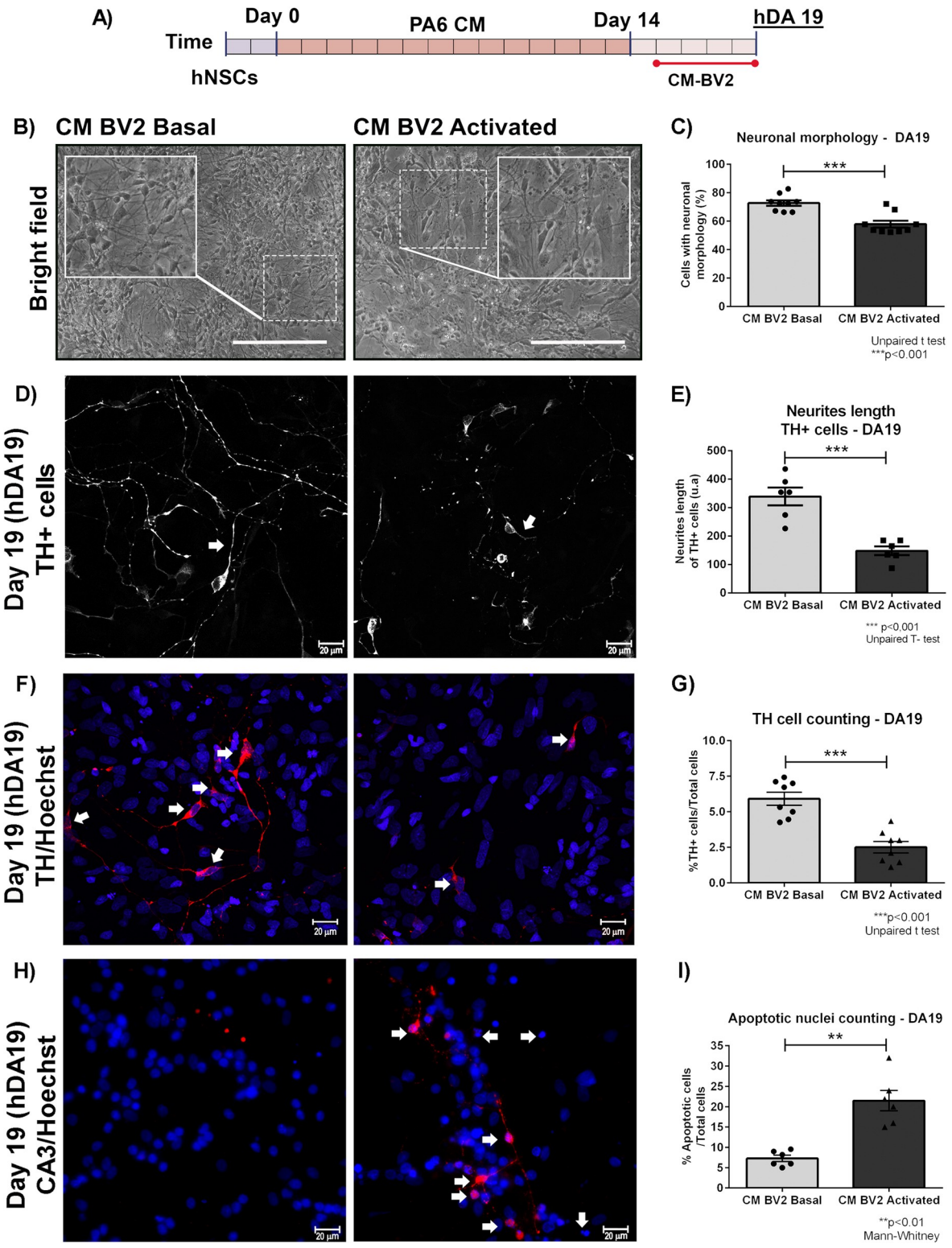

Fig 4. Effect of the activated microglia CM in the differentiation of DA precursors. (A) DA15 cultures were exposed to microglia CM (Basal or Activated) until day 19 (DA19). (B-E) For semi-quantitative analysis, photographs from independent experiments were analysed to determine neuron-like cell count and neurite length (arrows). Asterisks indicate statistically differences (***p<0.001. Unpaired T-test.) in percentage of neural-cell-like (n = 9) (C) and neurite length (n = 6) (E) of DA precursors cultured under inflammatory conditions (CM-BV2 activated) versus basal (CM-BV2 basal). There is a decrease in the number of cells with neuronal morphology and neurite length in DA precursors exposed with CM-BV2 activated. (F) Confocal images of TH-stained DA19 cell cultures. G) Asterisks indicate statistically

differences (***p<0.001. Unpaired T-test. n = 8) for cell counting assays of TH+ cells of DA precursors cultured with CM-BV2 activated versus basal (CM-BV2 basal). Arrowheads indicate TH+cells. (H-I) Cell death was analysed by fluorescence microscopy using Hoechst and detection of activated caspase 3 (CA3) by immunofluorescence. (H) Arrowheads indicate apoptotic nucleus and CA3-immunoreactive cell. An increment of CA3-positive cells (see indicator arrows) was observed in DA precursors incubated with CM-BV2 activated (40x magnification). (I) Asterisks show statistically significant differences (**p<0.01. Mann Whitney. n = 6) in DA precursors incubated with CM-BV2 activated versus CM-BV2 basal. Values are mean±SEM for the percentage of apoptotic cells relative to the total cell number. Scale bar are shown in white: 20μm. n = independent experiments.

https://doi.org/10.1371/journal.pone.0263021.g004

Conditioned media from microglia have toxic effects on hDAp: long term effects

In order to know if the short term effects after acute exposure to inflammatory conditions were transient or not, the protocol described before was carried out until DA19. Then, cell medium was replaced with PA6-CM (DA differentiation medium) and then, at the final stage of DA differentiation protocol (DA28), survival and morphological parameters were studied (Fig 5A). At DA28, a statistical reduction in the percentage of neuronal-like cells (CM-BV2 Basal: 89,6±2,9 vs. CM-BV2 Act: 64,5±3,9%. ***p<0,001) and neurite length (CM-BV2 Basal: 383,6±24,9 vs. CM-BV2 Act: 183,5±24,1. ***p<0,001) were detected in those cultures who were exposed for an acute period of time to a microglial activated-environment (CM-BV2 Activated) (Fig 5B–5E). Moreover, a reduction in the percentage of TUJ1-positive cells, in cell cultures exposed with CM-BV2 Activated was observed (CM-BV2 Basal: 54,0±3,1 vs. CM-BV2 Act: 29,8±0,9%TUJ1+cells. ***p<0,001) (Fig 8C and 8E). In addition, our results showed a significant decrease in the percentage of TH-positive cells in DA cultures treated with CM from activated BV2 (CM-BV2 Basal: 9,8±0,5 vs. CM-BV2 Act: 4,3±0,5%TH+cells. ***p<0,001) (Fig 5F and 5G). We conclude that there is no recovery of TH-positive cells in cultures initially incubated under inflammatory conditions.

Functional effects of TNF-α on survival and differentiation of DA precursors

Previously, the pro-inflammatory cytokine TNF-α was observed to be expressed after transplantation (Fig 2G), which was detected in cell culture supernatant of activated microglia (Fig 3B). Earlier studies reported cytotoxic effects of TNF-α in neural cell lines [22]. These findings lead us to study the role of TNF-α in the differentiation and survival of hDAp.

DA15 were cultured with CM-BV2 (basal or activated condition) during 4 days as previously described, with or without Etanercept (a TNF-α inhibitor) as co-treatment (Fig 6A). Neuronal differentiation was analysed by cell morphology and TUJ1-cell counting. Acute exposure to CM from activated microglia (CM-BV2 Act) affected cell morphology and TUJ1-positive cell percentage (CM-BV2 Basal: 43,9±1,4 vs. CM-BV2 Act: 30,3±1,4%TUJ1+cell. ***p<0,001), while TNF-α blockage was able to reverse neuronal loss (CM-BV2 Act+Etan: 40,9±1,7 vs. CM-BV2 Act: 30,3±1,4%TUJ1+cell. **p<0,01) (Fig 6B–6E).

In addition, Etanercept had no effects on the expression of TH when hDAp were incubated with CM from basal BV2 cells. However, inflammatory-mediated suppression of TH expression was overtly reversed by Etanercept co-treatment (CM-BV2 Act+Etan: 5,7±0,5 vs. CM-BV2 Act: 2,6±0,5%TH+cells. **p<0,01) (Fig 7B and 7E). Quantification of neurite length of DA19 indicated that, while pro-inflammatory conditions caused a decrease in neurite length, co-treatment with Etanercept reduced these alterations in TH-positive cells (Fig 7C and 7D). Finally, we measured cell death in DA19. Our results suggest that TNF-α mediated inhibition partially reduced the percentage of apoptotic cells (Fig 7F).

Similar effects of TNF-α inhibition were observed in all parameters studied previously at the terminal differentiation stage (DA28), suggesting a persistent protection of the hDAp after Etanercept treatment (Figs 8 and 9).

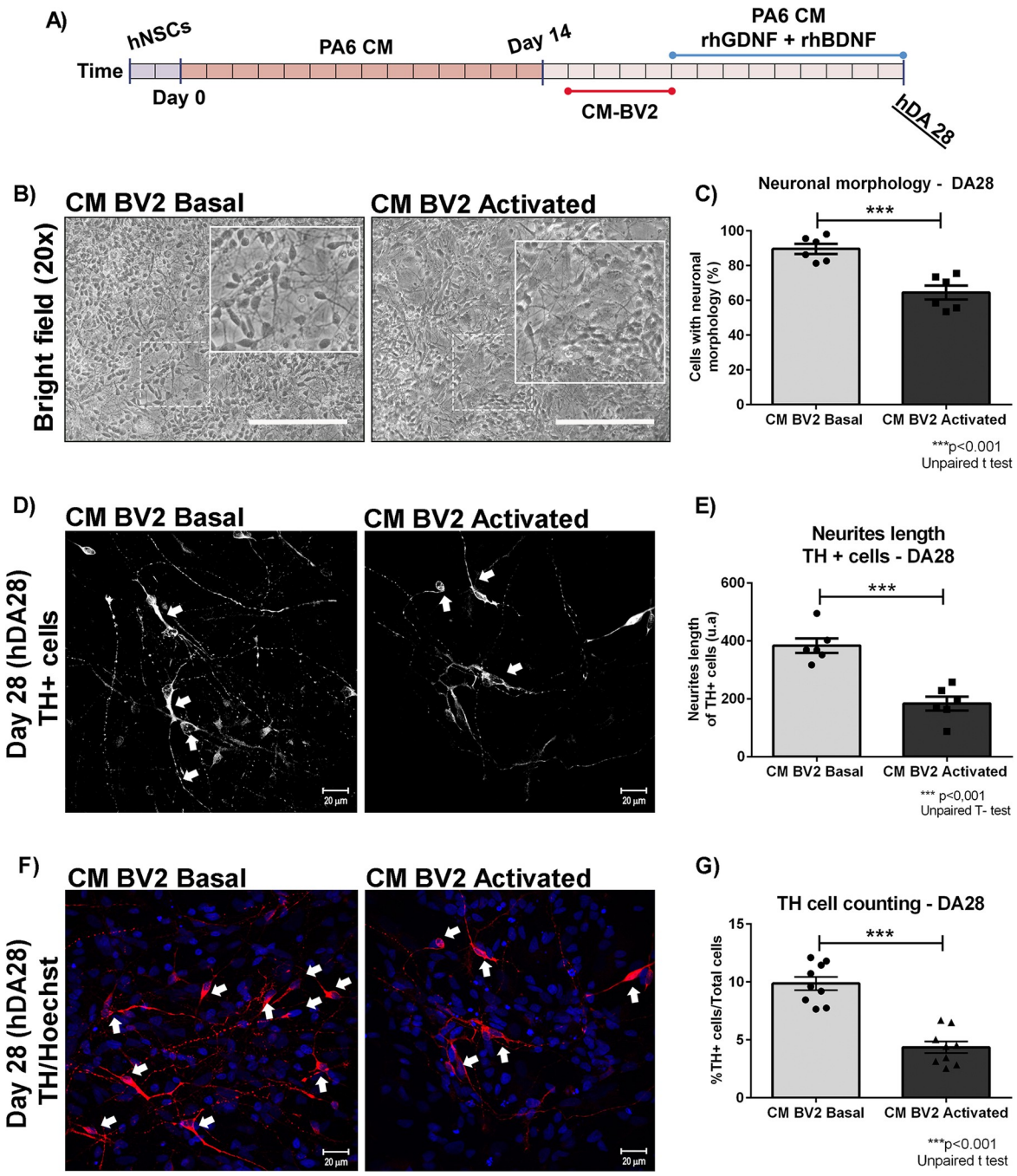

Fig 5. Impact of pro-inflammatory microenvironment on DA cultures. (A) CM from basal and activated conditions were added to DA precursors and incubated during 4 days. Morphological analysis and detection of DA neurons were performed at DA28. (B-E) For semi-quantitative analysis, photographs from independent experiments were analysed to study morphological alterations and determine neuron-like cell count (B) and neurite length (D). Asterisks indicate statistically significant differences at DA28 stage (***p<0.001. Unpaired T-test. n = 6) in the percentage of neural-cell-like (C) and neurite length of TH-positive cells (arrows) (***p<0.001. Unpaired T-test. n = 6) (E) of hDAp cells cultured under inflammatory conditions (CM-BV2 activated) versus basal (CM-BV2 basal). (F-G) Cell counting of TH-positive cells was performed. Representative photomicrographs from TH immunofluorescence (40x) of DA28 cells obtained from DA28 cultured with CM-BV-2 (basal and activated condition) are shown. Arrowheads indicate TH+cells. Asterisks indicate statistically significant differences (***p<0.001. Unpaired T-test. n = 9) for cell counting assays of TH+ cells of hDAp cultured under inflammatory conditions (CM-BV2 activated) versus basal microenvironment (CM-BV2 Basal) (G). Values are mean±SEM of n independent trials. Scale bar are shown in white: 20μm. n = independent experiments.

https://doi.org/10.1371/journal.pone.0263021.g005

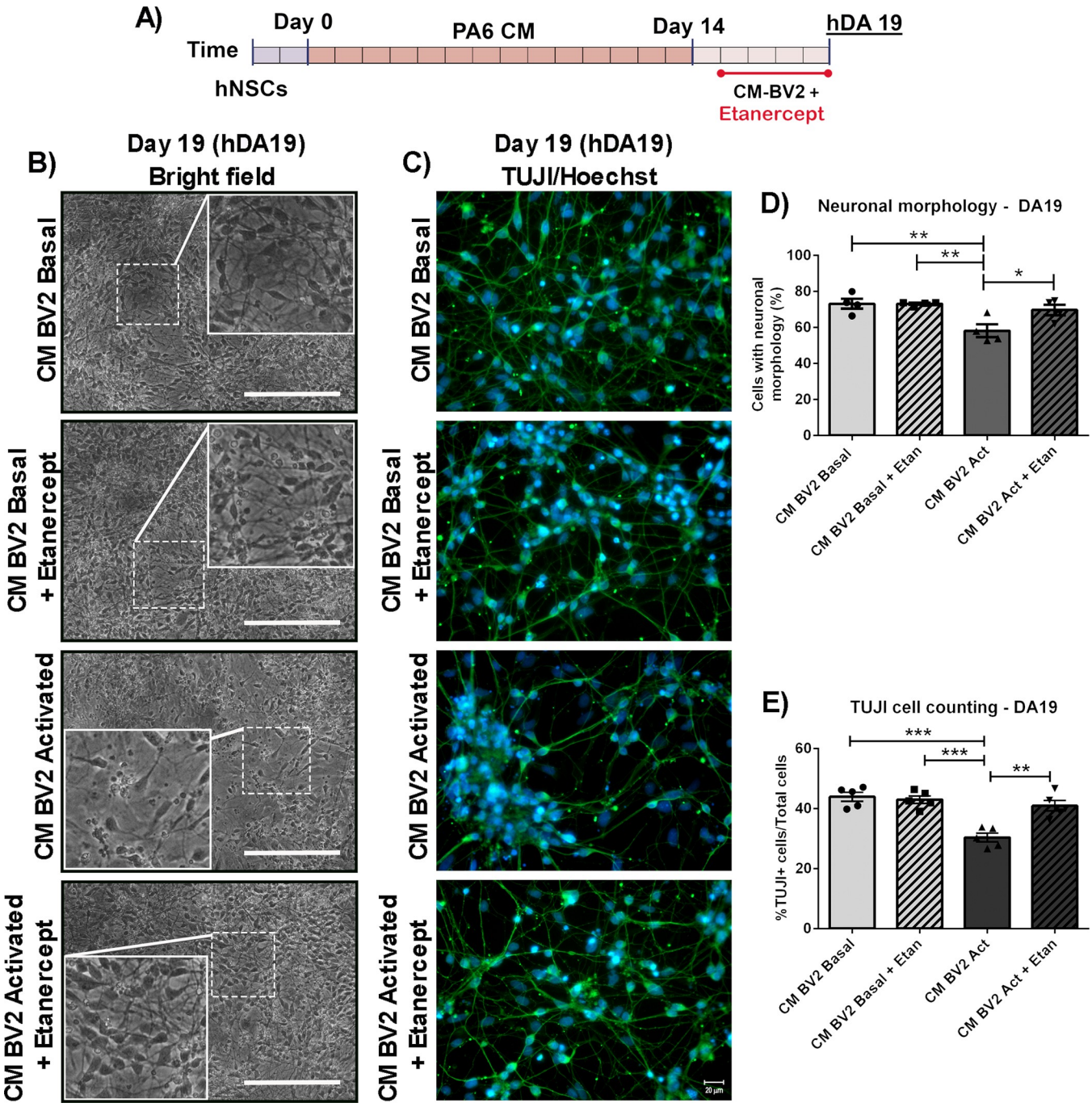

Fig 6. Effect of TNF-α inhibitor on differentiation of DA precursors exposed to activated microglia CM. (A) DA precursors were exposed with CM-BV2 during the 4 days, in the presence of Etanercept (a TNF-α inhibitor). (B) For semi-quantitative analysis, photographs from independent experiments were analysed to determine neuron-like cell count. (C) Detection of TUJ1+ cells by immunofluorescence and cell counting were performed at DA19. Photomicrographs are shown (40x). (D) Asterisks indicate statistically significant differences in percentage of neural-cell like DA precursors cultured under inflammatory conditions (CM-BV2 activated) versus basal (CM-BV2 basal) (*p<0.01 CM-BV2 Act vs. CM-BV2 Basal). Inhibition of TNF-α prevents the decrease in the number of cells with neuronal morphology (*p<0.05 CM-BV2 Act vs. CM-BV2 Act+Etan). ANOVA followed by Tukey's post hoc test. n = 4 independent assays. (E) Asterisks indicate statistically significant differences in percentages of TUJ1+ cells of hDAp cultured with CM from activated BV2 cultures versus CM from BV2 cells under basal conditions (***p<0.001 CM-BV2 Act vs. CM-BV2 Basal). Co-incubation of hDAp with Etanercept inhibited TUJ1+ cells diminution (**p<0.01 CM-BV2 Act vs. CM-BV2 Act+Etan). ANOVA followed by Bonferroni test. n = 5 independent assays. Values are means ± SEM of independent assays. Scale bar are shown in white: 20μm. n = independent experiments.

https://doi.org/10.1371/journal.pone.0263021.g006

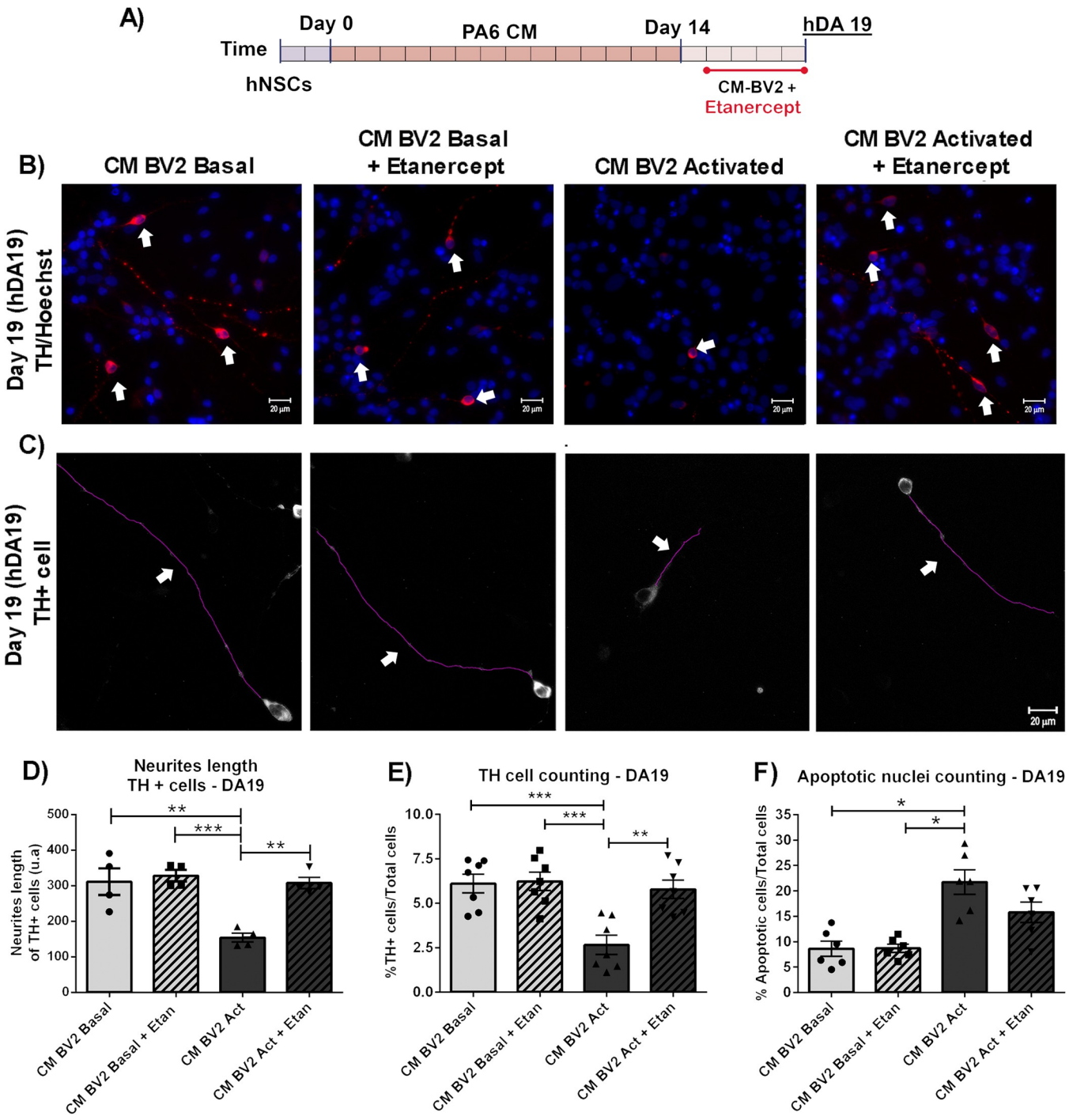

Fig 7. Effect of TNF-α inhibitor on survival and neurite length of DA precursors exposed to inflammatory conditions. (A) DA precursors were cultured in the presence of CM-BV2 (basal or activated condition) during 4 days, in the presence of Etanercept as co-treatment. (B) Detection of TH+cells (arrows) by immunofluorescence and cell counting were performed at DA19. Photomicrographs from immunofluorescence are shown (40x). (C) Neurite length analyses of TH+ cells were also performed at DA19. Photomicrographs are shown (40x). Arrowheads indicate neurites. (D) Decrease in neurite length were observed after exposure of DA precursors to activated CM-BV2 (**p<0.01 vs. CM-BV2 Basal). Inhibition of TNF-α reduces alterations in neurite length of TH+ cells (**p<0.01 CM-BV2 Act vs. CM-BV2 Act+Etanercept). ANOVA followed by Bonferroni test. n = 4. (E) Exposure of DA precursors to activated CM-BV2 decreased the percentage of TH+ cells (*** p <0.001 vs. CM-BV2 Basal). Inhibition of TNF-α prevents TH+ cell loss (**p<0.01 CM-BV2 Act vs. CM-BV2 Act +Etan. ANOVA followed by Bonferroni test. n = 7). (F) Cell death was analysed by apoptotic nucleus counting after Hoechst staining. The results showed that exposure of DA precursors to CM- from activated microglia significantly increase in cell death (*p<0.05 vs. CM-BV2 Basal. Kruskal-Wallis one way ANOVA followed by Dunn's test. n = 7). Partial reduction of apoptotic cells are detected in cell culture treated with Etanercept. Values are means±SEM of independent assays. Scale bar are shown in white: 20μm. n = independent experiments.

https://doi.org/10.1371/journal.pone.0263021.g007

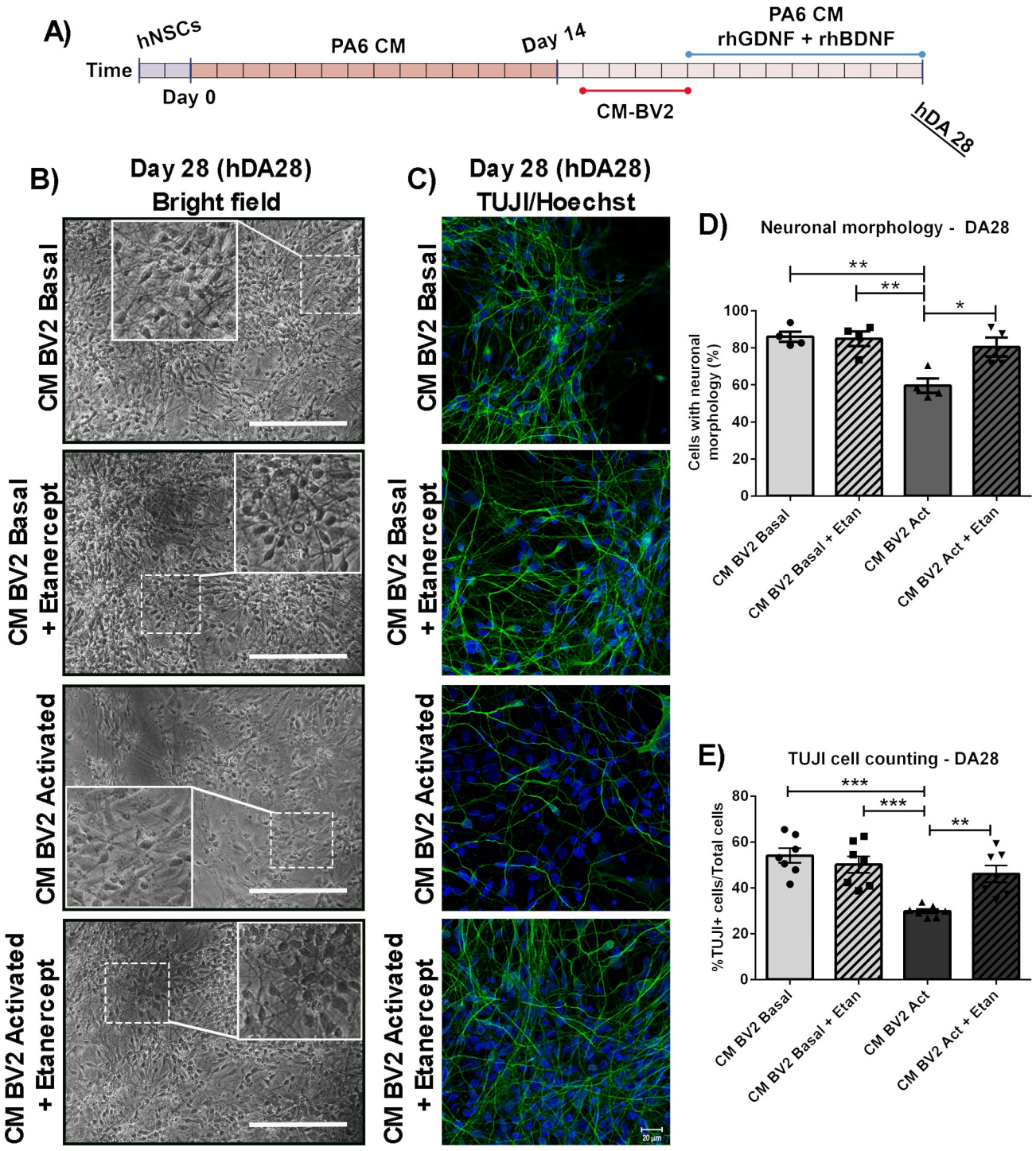

Fig 8. Inhibition of TNF-α and final differentiation of DA precursors exposed to proinflammatory conditions. (A) DA precursors were exposed with CM-BV2 (basal or activated condition) during the 4 days, in the presence of Etanercept. At DA19, cell media was changed to PA6-CM. Morphological assay and detection of TUJ1+ cells by immunofluorescence were performed at DA28. (B, D) For semi-quantitative analysis, photographs from independent experiments were analysed to determine neuron-like cell count. Asterisks indicate statistically significant differences in percentage of neural-cell-like of DA precursors cultured under inflammatory conditions (CM-BV2 activated) versus basal (CM-BV2 basal) (**p<0.01 CM-BV2 Act vs. CM-BV2 Basal). Inhibition of TNF-α prevents the decrease in the number of cells with neuronal morphology (*p<0.05 CM-BV2 Act vs. CM-BV2 Act +Etan). ANOVA followed by Tukey's post hoc test. n = 4. (C, E) Photomicrographs from TUJ1 immunofluorescence (40x) of DA28 cultures are shown. Asterisks indicate statistically significant differences in percentages of TUJ1+ cells of DA cultures exposed with CM from activated BV2 cultures versus CM from BV2 cells under basal conditions (***p<0.001 CM-BV2 Act vs. CM-BV2 Basal). Co-incubation of DA cell cultures with Etanercept inhibited TUJ1+ cells diminution (**p<0.01 CM-BV2 Act vs. CM-BV2 Act+Etan.) (n = 7 independent assays). ANOVA followed by Bonferroni test. Values are means±SEM of independent assays. Scale bar are shown in white: 20μm. n = independent experiments.

https://doi.org/10.1371/journal.pone.0263021.g008

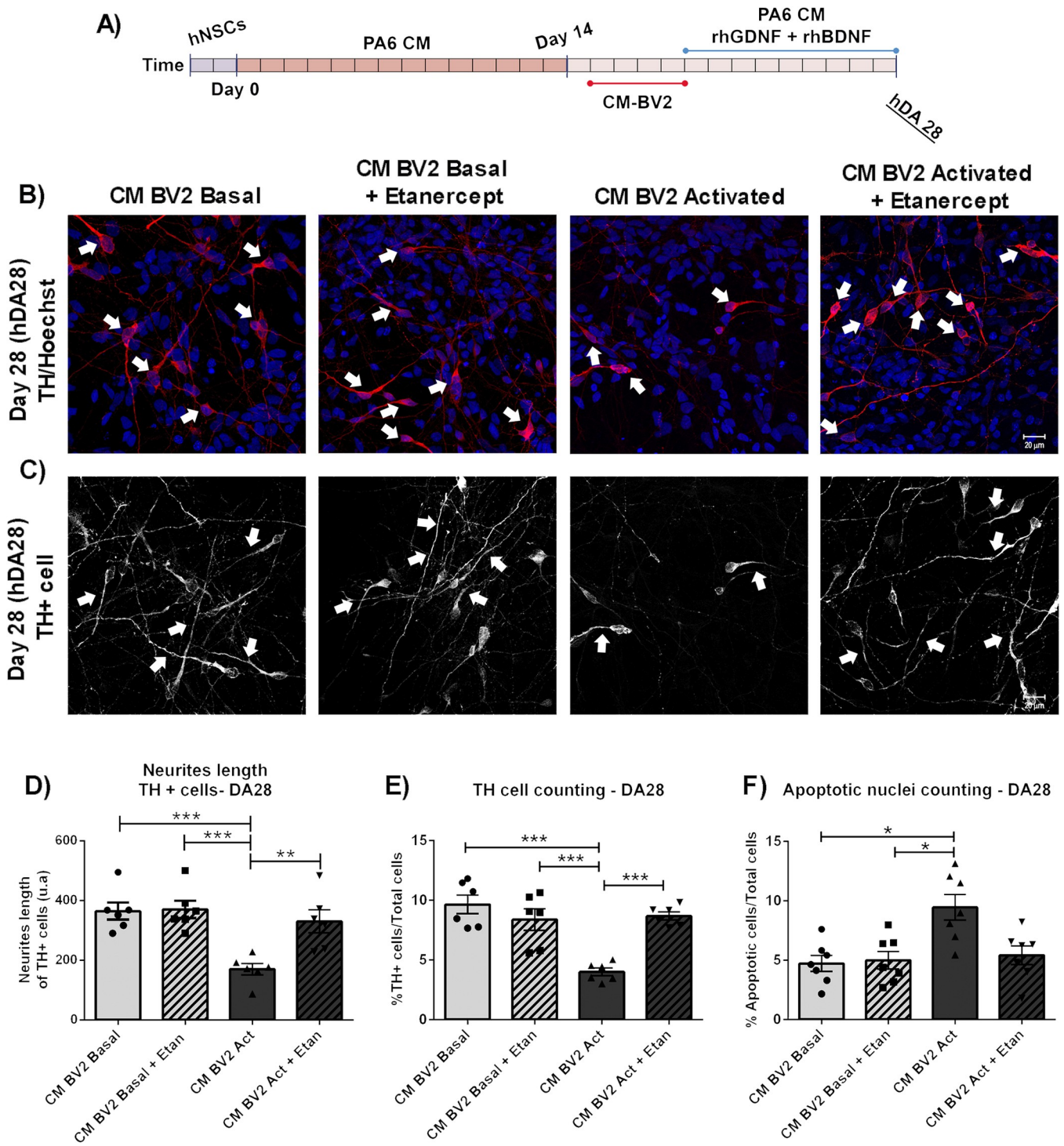

Fig 9. Long term study of Etanercept effect on DA cultures exposed to acute inflammatory conditions. (A) DA precursors were cultured in the presence of CM-BV2 (basal or activated condition) during the 4 days. A co-treatment of DA precursors with CM-BV2 and Etanercept were performed. (B-C) At DA28, immunofluorescence against the dopaminergic marker TH and neurite length analyses were performed. Arrowheads indicate TH+cells (B) and neurites (C). Cell death was analysed by apoptotic nuclei counting after Hoechst staining. Photomicrographs from immunofluorescence are shown (40x). (D) Diminution in neurite length were observed in DA cultures incubated to CM from activated BV2 (***$p<0.001$ CM-BV2 Act vs. CM-BV2 Basal). Inhibition of TNF-α reduces alterations in neurite length of DA cells (**$p<0.01$ CM-BV2 Act vs. CM-BV2 Act+Etan. ANOVA followed by Bonferroni test. n = 6)). E) Acute exposure of DA precursors to CM from activated microglia decreased the final percentage of TH+ cells (***$p<0.001$ CM-BV2 Act vs. CM-BV2 Basal). Etanercept co-incubation was able to prevent TH+ cell loss (***$p<0.001$ CM-BV2 Act vs. CM-BV2 Act+Etan. ANOVA followed by Bonferroni test). (F) The results from cell death analyses show that acute exposure of DA precursors to CM- from activated microglia increase in cell death (*$p<0.05$ vs. CM-BV2 Basal. Kruskal-Wallis

one-way ANOVA followed by Dunn's test. n = 7). Etanercept was able to reduce the percentage of apoptotic cells. Values are mean±SEM of n independent assays. Scale bar are shown in white: 20μm. n = independent experiments.

https://doi.org/10.1371/journal.pone.0263021.g009

Discussion

Cell replacement therapy involves disruption of the blood–brain barrier (BBB) and host tissue damage, which cause astrocyte and microglia activation [23,24]. Therefore, grafted cells are surrounded by an altered environment where host tissue signals could affect relevant processes for the efficacy of cell therapy, such as survival and differentiation of DA precursors.

In this study, we have investigated for the first time the short-term response of the cerebral parenchyma to human DA precursors (hDAp) transplantation and further studied the effects of the microglia response on hDAp viability and differentiation *in vitro*. We show that a glial response was sustained in time after transplantation, together with TNF-α expression, under immunosuppression conditions. *In vitro*, acute exposure to conditioned media (CM) from activated microglia diminished the percentage of TH positive cells, induced cell death and affected the differentiation process. In addition, this acute pro-inflammatory treatment of hDAp had a negative impact on terminal differentiation. Finally, specific inhibition of TNF-α reduced the loss of hDAp and the alterations in morphology.

In our *in vivo* model, a short-term host primary response related to the grafted hDAp (DA14) was detected with a significant increase of host MHCII- and GFAP-positive cells in adult immunosuppressed male rats. These observations were supported using other cell types who demonstrated an early increase in Iba1- and GFAP-positive cells following a NSC graft, until day 3 post-surgery [24]. Further support to our observations come from work by Tomov and colleagues who observed microglia and GFAP-positive cells between 7 and 28 days after allogeneic transplantation of ventral mesencephalic (VM) cells in a rodent model of PD [6,25]. In addition, MHCII-positive cells around hDAp grafts derived from iPSCs were detected long-term in a PD model of immunosuppressed non-human primates [26]. At the molecular level, we observed expression of the pro-inflammatory cytokine TNF-α in host-microglia (ED-1)-positive cells after transplantation with hDAp. Interestingly, TNF-α was also detected in the acute period following VM neuroblasts allogeneic grafts from rodents [27] and in allogeneic and xenogeneic transplantation of VM neuroblasts from rodents and pigs, respectively [28]. Therefore, our data extend and support previous observations on an early host response after brain grafting of other cell types and animal models. Taken together, we preliminary conclude that there seems to be no overt specificity on the host innate immune response to different transplanted cell types at the cellular level.

In contrast with our results, Tiklova and colleagues have performed a thorough scRNA analysis after cell transplantation [29]. These different results between that work and ours could be related to the time of analysis. While their work analyzed animals after 6 months' post-transplantation, our experiments were analyzed 28 days post-grafting. This is an important difference since the innate immune response is usually short lasting. In the case this hypothesis holds true, it suggests that the possible time window of intervention to affect the host response via immunosuppression may be soon after transplantation.

We have also developed an in vitro approach which partially simulates the pro-inflammatory microenvironment from the host response related to the graft. This system is based on exposure of hDAp derived from human NSCs to conditioned media from LPS-activated BV-2 microglial cells at short-(DA19) and long-term (DA28) end points. Previous research has demonstrated that BV2 cells are a valid model of microglia culture and their exposure to LPS is widely used to study microglial activation to a pro-inflammatory state [30]. But, since the host

response to cell transplantation is not fully characterized, this approach only provides a close experimental model to the in vivo paradigm. In addition, rodent TNF can activate human TNFRI and TNFRII [31]. Other microglial models such as primary microglial cultures or human iPSC-derived microglia could be used in future experiments to test similar hypotheses as in this work.

Our results showed a significant increase in cell death of DA precursors exposed with CM from activated microglia by means of a decrease in TH-positive cells in early and late cell culture stages. Our data on cell death extend similar effects of CM from activated microglia observed in other cell types such as SH-SY5Y and PC12 cultures [12,17]. Previous reports suggest that the crosstalk between the Bcl family and NF-κB could be involved in DAn vulnerability [32,33]. The functional role of these molecules required further analyses.

We also observed morphological alterations specifically induced by CM from activated microglia, such as a decrease in neuron-like cells and neurite length of TH-positive cells at both stages of DA differentiation. Moreover, the percentage of TUJ1-positive cells, a pan-neuronal marker, was diminished by microglia activation. Interestingly, using human cortical neural progenitor cells, TNF-α treatment during six days reduced TUJ1 percentage and increased GFAP-positive cells, suggesting that this cytokine inhibited neuronal differentiation [34]. Altogether, our results and others indicate that activated microglial cells and TNF-α could play a role in the survival and differentiation of hDAp and other cells after transplantation.

From the evidence obtained *in vivo*, we were interested in analysing the effect of TNF-α on hDAp. Co-treatment of activated CM with Etanercept, a TNF-α inhibitor, was able to reverse the reduction of TH-positive cells, cell death and morphological alterations previously observed in hDAp. These results extend a previous finding which reported that inhibition of TNF-α reversed the reduction of DA markers and morphological alterations in other cells such as human TH-positive cells derived from Synovial adipose stem cells [35].

As we mentioned above, none of the current PD therapies stops neurodegeneration or functionally replaces dopaminergic neuronal loss. Currently, a remarkable effort is being made in order to take cell replacement therapy for PD to the clinic (5). Recently, in 2018, the first clinical trial using GMP-grade hDAp derived from iPSCs was launched, a case report of autologous-cell therapy for PD was published last year and a phase 1 study to evaluate pluripotent stem cell-derived hDAp in patients with PD was approved by the regulatory authorities of US [36,37]. Survival, differentiation and integration of the transplanted precursors are biological processes that could influence the effectiveness of this strategy and are affected by the host response [23].

In particular, a major limiting factor of cell replacement therapy for PD is still the poor survival rate (10%) of grafted DA precursors [38]. Our study points to TNF-α inhibition as a possible strategy to increase survival and differentiation of grafted hDAp. It remains to be determined whether the sole inhibition of TNF or any of its receptors after transplantation is necessary and sufficient to inhibit the deleterious effects of inflammation as we have observed *in vitro*. Nevertheless, several TNF-α inhibitors are clinically available for other diseases. A possible strategy that could be used is the transplantation of DA precursors along with co-infusion of a TNF inhibitor or monoclonal antibodies since inhibitors against TNF-α such as Etanercept and TNF-R1 antagonist as ATROSAB cannot cross BBB under physiological conditions. Alternatively, since cell transplantation includes temporal BBB disruption, treatment with agents to neutralise TNF-α deleterious action could be used immediately after surgery. On the other hand, the peripheral administration of a soluble TNF-α inhibitor (XPro1595) was neuroprotective on an *in vivo* model of PD [39]. Then, molecules such as XPro1595 could be good candidates to be used in animal's models of cell replacement therapy for PD in order to analyse its potential in this specific strategy.

In addition, it has been recently shown the relevance of TNF -α expression after transplantation using a different approach [40]. Using a pooled CRISPR/Cas9 screen to enhance survival of dopamine neurons in vivo, TNF-α signaling was causally link to inhibition in cell survival [40]. Furthermore, cell sorting with a widely used, clinically approved TNF-α inhibitor, enabled efficient engraftment and functional recovery in a preclinical PD mouse model. This work concludes that transient TNF-α inhibition presents a clinically relevant strategy to enhance survival and engraftment of human PSC-derived dopamine neurons in PD. Therefore, this recent work supports the claims from our study using a completely different approach and provide functional evidence of the role of the TNF-α expression we have observed after transplantation. We believe that the novel *in vitro* data we provide complements and strengthens the data from the paper described and paves the way for new exploration on the mechanism of the functional role of TNF-α on cell survival after transplantation.

In conclusion, our data indicate that microglia-derived TNF-α may play a key role in the possible effects of the host response to hDAp transplantation by affecting survival and differentiation at short and long-term. Selective targeting of TNF-α may hold translational potential to increase survival and differentiation of DA precursors even under immunosuppressive treatments targeting the adaptive immune response. Finally, the *in vitro* model described might be useful to study the mechanism of action of microglia on hDAp and search for potential anti-inflammatory and/or neuroprotective treatments that may improve survival and differentiation efficacy of hDAp.

Supporting information

S1 Fig. Representative images of the graft stained with Cresyl Violet. 24 hs and 7 days post-surgery (Day 1). On day 1, grafts presented an increase of PMN neutrophils (arrows) compared with samples after 7 days (Day 7) post transplantation (Magnification: 100X). Inset: Digital inset where PMN can be observed (arrows). B. No expression of Interleukin (IL)-1 beta or IL-6 was observed at Day 28 post-transplantation by immunofluorescence. Negative control: Similar brain samples but omitting the primary antibody. Positive controls: Samples from brains expressing IL-1 beta (green) and IL-6 (red), treated as described in Materials and Methods. Representative pictures of the grafts are shown (Magnification: 40X). Scale bar are shown in white: 20μm. n = independent experiments.
(TIF)

S1 File.
(XLSX)

Author Contributions

Conceptualization: María Celeste Leal, Fernando J. Pitossi.

Formal analysis: Shirley D. Wenker, Fernando J. Pitossi.

Funding acquisition: Shirley D. Wenker, Fernando J. Pitossi.

Investigation: Shirley D. Wenker, María Isabel Farias, Victoria Gradaschi, Corina Garcia, Juan Beauquis, María Celeste Leal, Carina Ferrari.

Methodology: Shirley D. Wenker, María Isabel Farias, Victoria Gradaschi, Corina Garcia, Juan Beauquis, María Celeste Leal, Carina Ferrari.

Project administration: Shirley D. Wenker, Fernando J. Pitossi.

Resources: Xianmin Zeng.

Writing – original draft: Shirley D. Wenker, Fernando J. Pitossi.

Writing – review & editing: Shirley D. Wenker, Corina Garcia, María Celeste Leal, Carina Ferrari, Fernando J. Pitossi.

References

1. Dorsey ER, Bloem BR. The Parkinson Pandemic—A Call to Action. JAMA Neurol. 2018 Jan 1; 75(1). https://doi.org/10.1001/jamaneurol.2017.3299 PMID: 29131880
2. Coelho M, Ferreira JJ. Late-stage Parkinson disease. Nat Rev Neurol. 2012 Aug 10; 8(8). https://doi.org/10.1038/nrneurol.2012.126 PMID: 22777251
3. Wenker SD, Leal MC, Farías MI, Zeng X, Pitossi FJ. Cell therapy for Parkinson′s disease: Functional role of the host immune response on survival and differentiation of dopaminergic neuroblasts. Brain Res. 2016 May;1638. https://doi.org/10.1016/j.brainres.2015.06.054 PMID: 26239914
4. Brundin P, Strecker RE, Widner H, Clarke DJ, Nilsson OG, Astedt B, et al. Human fetal dopamine neurons grafted in a rat model of Parkinson's disease: immunological aspects, spontaneous and drug-induced behaviour, and dopamine release. Exp Brain Res. 1988; 70(1):192–208. https://doi.org/10.1007/BF00271860 PMID: 3402564
5. Parmar M, Grealish S, Henchcliffe C. The future of stem cell therapies for Parkinson disease. Nat Rev Neurosci. 2020 Feb 6; 21(2). https://doi.org/10.1038/s41583-019-0257-7 PMID: 31907406
6. Tomov N, Surchev L, Wiedenmann C, Döbrössy MD, Nikkhah G. Astrogliosis has Different Dynamics after Cell Transplantation and Mechanical Impact in the Rodent Model of Parkinson's Disease. Balkan Med J. 2018 Mar 15; 35(2). https://doi.org/10.4274/balkanmedj.2016.1911 PMID: 29039346
7. Hassanzadeh K, Rahimmi A. Oxidative stress and neuroinflammation in the story of Parkinson's disease: Could targeting these pathways write a good ending? J Cell Physiol. 2019 Jan; 234(1).
8. Swistowski A, Peng J, Liu Q, Mali P, Rao MS, Cheng L, Zeng X. Efficient generation of functional dopaminergic neurons from human induced pluripotent stem cells under defined conditions. Stem Cells. 2010 Oct; 28(10). https://doi.org/10.1002/stem.499 PMID: 20715183
9. Peng J., Liu Q., Rao MS., and Zeng X. Survival and engraftment of dopaminergic neurons manufactured by a GMP-compatible process. Cytotherapy. 2014 Sep; 16(9).
10. Swistowska AM, da Cruz AB, Han Y, Swistowski A, Liu Y, Shin S, Zhan M, Rao MS, Zeng X. Stage-specific role for shh in dopaminergic differentiation of human embryonic stem cells induced by stromal cells. Stem Cells Dev. 2010 Jan; 19(1):71–82. https://doi.org/10.1089/scd.2009.0107 PMID: 19788370
11. Liu Q, Pedersen OZ, Peng J, Couture LA, Rao MS, Zeng X. Optimizing dopaminergic differentiation of pluripotent stem cells for the manufacture of dopaminergic neurons for transplantation. Cytotherapy. 2013 Aug; 15(8). https://doi.org/10.1016/j.jcyt.2013.03.006 PMID: 23664011
12. Dai X, Li N, Yu L, Chen Z, Hua R, Qin X, et al. Activation of BV2 microglia by lipopolysaccharide triggers an inflammatory reaction in PC12 cell apoptosis through a toll-like receptor 4-dependent pathway. Cell Stress Chaperones. 2015 Mar 12; 20(2). https://doi.org/10.1007/s12192-014-0552-1 PMID: 25387796
13. Paxinos G, Watson C. The rat brain in stereotaxic coordinates. Orlando, FL: Academic Press; 1986.
14. Brüstle O, Cunningham MG, Tabar V, Studer L. Experimental Transplantation in the Embryonic, Neonatal, and Adult Mammalian Brain. Curr Protoc Neurosci. 1997 Nov; 1(1).
15. Jensen MB, Krishnaney-Davison R, Cohen LK, Zhang S-C. Injected Versus Oral Cyclosporine for Human Neural Progenitor Grafting in Rats. J Stem Cell Res Ther. 2012;01(S10). https://doi.org/10.4172/2157-7633.S10-003 PMID: 24765542
16. Papazian I, Kyrargyri V, Evangelidou M, Voulgari-Kokota A, Probert L. Mesenchymal Stem Cell Protection of Neurons against Glutamate Excitotoxicity Involves Reduction of NMDA-Triggered Calcium Responses and Surface GluR1, and Is Partly Mediated by TNF. Int J Mol Sci. 2018 Feb 25; 19(3). https://doi.org/10.3390/ijms19030651 PMID: 29495345
17. Wenker SD, Chamorro ME, Vittori DC, Nesse AB. Protective action of erythropoietin on neuronal damage induced by activated microglia. FEBS J. 2013 Apr; 280(7). https://doi.org/10.1111/febs.12172 PMID: 23384249
18. Silva BA, Leal MC, Farías MI, Erhardt B, Galeano P, Pitossi FJ et al Environmental enrichment improves cognitive symptoms and pathological features in a focal model of cortical damage of multiple sclerosis. Brain Res. 2020 Jan 15; 1727:146520. https://doi.org/10.1016/j.brainres.2019.146520 PMID: 31669283

19. López-Carballo G, Moreno L, Masiá S, Pérez P, Barettino D. Activation of the Phosphatidylinositol 3-Kinase/Akt Signaling Pathway by Retinoic Acid Is Required for Neural Differentiation of SH-SY5Y Human Neuroblastoma Cells. J Biol Chem. 2002 Jul; 277(28). https://doi.org/10.1074/jbc.M201869200 PMID: 12000752

20. Bonafina A, Fontanet PA, Paratcha G, Ledda F. GDNF/GFRα1 Complex Abrogates Self-Renewing Activity of Cortical Neural Precursors Inducing Their Differentiation. Stem Cell Reports. 2018 Mar; 10 (3).

21. Pott Godoy MC, Ferrari CC, Pitossi FJ. Nigral neurodegeneration triggered by striatal AdIL-1 administration can be exacerbated by systemic IL-1 expression. J Neuroimmunol. 2010; 222(1–2). https://doi.org/10.1016/j.jneuroim.2010.02.018 PMID: 20350768

22. Pregi N, Wenker S, Vittori D, Leirós CP, Nesse A. TNF-alpha-induced apoptosis is prevented by erythropoietin treatment on SH-SY5Y cells. Exp Cell Res. 2009 Feb; 315(3). https://doi.org/10.1016/j.yexcr.2008.11.005 PMID: 19056379

23. Salado-Manzano C, Perpiña U, Straccia M, Molina-Ruiz FJ, Cozzi E, Rosser AE, et al. Is the Immunological Response a Bottleneck for Cell Therapy in Neurodegenerative Diseases? Front Cell Neurosci. 2020 Aug 11; 14. https://doi.org/10.3389/fncel.2020.00250 PMID: 32848630

24. Hoornaert CJ, Le Blon D, Quarta A, Daans J, Goossens H, Berneman Z, et al. Concise Review: Innate and Adaptive Immune Recognition of Allogeneic and Xenogeneic Cell Transplants in the Central Nervous System. Stem Cells Transl Med. 2017 May; 6(5). https://doi.org/10.1002/sctm.16-0434 PMID: 28244236

25. Tomov N, Surchev L, Wiedenmann C, Döbrössy M, Nikkhah G. Roscovitine, an experimental CDK5 inhibitor, causes delayed suppression of microglial, but not astroglial recruitment around intracerebral dopaminergic grafts. Exp Neurol. 2019 Aug; 318.

26. Kikuchi T, Morizane A, Doi D, Magotani H, Onoe H, Hayashi T, et al. Human iPS cell-derived dopaminergic neurons function in a primate Parkinson's disease model. Nature. 2017 Aug 31; 548(7669).

27. Clarke DJ, Branton RL. A Role for Tumor Necrosis Factor α in Death of Dopaminergic Neurons Following Neural Transplantation. Exp Neurol. 2002 Jul; 176(1).

28. Mirza B, Krook H, Andersson P, Larsson LC, Korsgren O, Widner H. Intracerebral cytokine profiles in adult rats grafted with neural tissue of different immunological disparity. Brain Res Bull. 2004 Mar; 63 (2). https://doi.org/10.1016/j.brainresbull.2004.01.009 PMID: 15130699

29. Tiklová K, Nolbrant S, Fiorenzano A, Björklund ÅK, Sharma Y, Heuer A, Gillberg L, Hoban DB, Cardoso T, Adler AF, Birtele M, Lundén-Miguel H, Volakakis N, Kirkeby A, Perlmann T, Parmar M. Single cell transcriptomics identifies stem cell-derived graft composition in a model of Parkinson's disease. Nat Commun. 2020 May 15; 11(1).

30. Henn A, Lund S, Hedtjärn M, Schrattenholz A, Pörzgen P, Leist M. The suitability of BV2 cells as alternative model system for primary microglia cultures or for animal experiments examining brain inflammation. Vol. 26, Altex. 2009. https://doi.org/10.14573/altex.2009.2.83 PMID: 19565166

31. Bossen C, Ingold K, Tardivel A, Bodmer J-L, Gaide O, Hertig S, et al. Interactions of Tumor Necrosis Factor (TNF) and TNF Receptor Family Members in the Mouse and Human. J Biol Chem. 2006 May; 281(20). https://doi.org/10.1074/jbc.M601553200 PMID: 16547002

32. Bellucci A, Bubacco L, Longhena F, Parrella E, Faustini G, Porrini V, et al. Nuclear Factor-κB Dysregulation and α-Synuclein Pathology: Critical Interplay in the Pathogenesis of Parkinson's Disease. Front Aging Neurosci. 2020 Mar 24; 12.

33. Seiz EG, Ramos-Gómez M, Courtois ET, Tønnesen J, Kokaia M, Liste Noya I, et al. Human midbrain precursors activate the expected developmental genetic program and differentiate long-term to functional A9 dopamine neurons in vitro. Enhancement by Bcl-XL. Exp Cell Res. 2012 Nov; 318(19).

34. Lan X, Chen Q, Wang Y, Jia B, Sun L, Zheng J, et al. TNF-α Affects Human Cortical Neural Progenitor Cell Differentiation through the Autocrine Secretion of Leukemia Inhibitory Factor. PLoS One. 2012 Dec 7; 7(12).

35. Herrmann M, Anders S, Straub RH, Jenei-Lanzl Z. TNF inhibits catecholamine production from induced sympathetic neuron-like cells in rheumatoid arthritis and osteoarthritis in vitro. Sci Rep. 2018 Dec 25; 8 (1). https://doi.org/10.1038/s41598-018-27927-8 PMID: 29941879

36. Takahashi J. iPS cell-based therapy for Parkinson's disease: A Kyoto trial. Regen Ther. 2020 Mar; 13. https://doi.org/10.1016/j.reth.2020.06.002 PMID: 33490319

37. Takahashi J. Clinical Trial for Parkinson's Disease Gets a Green Light in the US. Cell Stem Cell. 2021 Feb; 28(2).

38. Brundin P, Karlsson J, Emgård M, Schierle GSK, Hansson O, Petersén Å, et al. Improving the Survival of Grafted Dopaminergic Neurons: A Review over Current Approaches. Cell Transplant. 2000 Mar 22; 9 (2). https://doi.org/10.1177/096368970000900205 PMID: 10811392

39. Fischer R, Kontermann RE, Pfizenmaier K. Selective Targeting of TNF Receptors as a Novel Therapeutic Approach. Front Cell Dev Biol. 2020 May 26;8. https://doi.org/10.3389/fcell.2020.00401 PMID: 32528961

40. Kim TW, Koo SY, Riessland M, Cho H, Chaudhry F, Kolisnyk B, et al. TNF-NFkB-p53 axis restricts *in vivo* survival of hPSC-derived dopamine neuron. bioRxiv. 2023 Mar 31:2023.03.29.534819. https://doi.org/10.1101/2023.03.29.534819 PMID: 37034664